

# Automatic Sitting Pose Generation for Ergonomic Ratings of Chairs

Aihua Mao, Hong Zhang, Zhenfeng Xie, Minjing Yu, Yong-Jin Liu<sup>ID</sup>, Senior Member, IEEE, and Ying He<sup>ID</sup>

**Abstract**—Human poses play a critical role in human-centric product design. Despite considerable researches on pose synthesis and pose-driven product design, most of them adopt the simple stick figure model that captures only skeletons rather than real body geometries and do not link human poses to the environment (e.g., chairs for sitting). This paper focuses on user-tailored ergonomic design and rating of chairs using scanned human geometries. Fully utilizing the anthropometric information of the human models, our method considers more ergonomic guidelines of chair design (such as pressure distribution and support intensity) and links the geometry of 3D chair models and human-to-chair interactions into the pose deformation constraints of the human avatars. The core of our method is a pose generation algorithm which rigs the user's successive poses through coarse- and fine-level pose deformations. We define a non-linear energy function with contact, collision, and joint limit terms, and solve it using a hill-climbing algorithm. The fitting results allow us to quantitatively evaluate the chair model in terms of various ergonomic criteria. Our method is flexible and effective and can be applied to users with varying body shapes and a wide range of chairs. Moreover, the proposed technique can be easily extended to other furniture, such as desk, bed, and cabinet. Extensive evaluations and a user study demonstrate the efficiency and advantages of the proposed virtual fitting method. Given that our method avoids tedious on-site trying, facilitates the exploration/evaluation of various chair products, and provides valuable feedback for the designers and manufacturers to deliver customized products, it is ideal for online shopping of chairs.

**Index Terms**—Sitting pose generation, alignment, human-chair interaction, ergonomic rating

## 1 INTRODUCTION

ONLINE shopping is now a mainstream activity. E-Commerce offers great choice and convenience — giving customers the ability to shop from anywhere and anytime they want. Since customers make direct purchases online and do not set foot into shops, a potential risk is that the product, though looking perfect on a computer screen, does not fit their requirement due to unmatched sizes. For online cloth shopping, there are many virtual try-on tools that allow customers to visually examine whether the clothes fit. However, purchasing furniture (such as a chair) is a more complicated decision making process, since customers consider not only the physical dimension and the functionality, but also the ergonomic criteria. There is also an increasing demand for customized products that are safer and more comfortable than the one-size-fits-all products. Unfortunately, without a reliable virtual evaluation method,

customers still feel it necessary to visit the retail shops before making their decisions.

This paper aims at overcoming the above-mentioned challenge by developing a method for the user-tailored ergonomic rating of chairs. Our method considers the anthropometric and biomechanical characteristics of the human bodies, fits the geometry of the customer's body to the chairs and evaluates its functionality and measures its ergonomic performance. In contrast to the existing researches that commonly adopt a simple stick figure model to represent humans, our method takes scanned human bodies as input. We utilize the reconstructed 3D avatars of individuals and rig the pose of avatars to fit the 3D chairs. The final rigged pose of the avatar is determined by the geometries of chairs and ergonomic-guided contact constraints. We then compute an ergonomic score for the 3D models according to the fitting extent considered in terms of geometrical fit, pressure distribution, and support area.

This work is desired for furniture vendors to promote their products and for customers to explore and find the ideal chair without on-site trying. Thanks to the real geometries used, our method allows users to visually examine how their avatars interact with the chair and quantitatively evaluate the ergonomic scores. Such feedback is also valuable to the designers to develop and improve customized chairs. To the best of our knowledge, this is the first work to provide virtual experience of chair models based on the realistic human body. Our method can also be extended to other furniture by considering their functionality and ergonomic constraints. See Fig. 1 for two examples generated by our method.

- A.H. Mao, H. Zhang, and Z.F. Xie are with the School of Computer Science and Engineering, South China University of Technology, Guangzhou 510006, China. E-mail: {ahmao, 201620131291, 201720140063}@scut.edu.cn.
- M. Yu is with the College of Intelligence and Computing, Tianjin University, Tianjin 300350, China. E-mail: minjingyu@tju.edu.cn.
- Y.-J. Liu is with BNRIst, MOE Key Laboratory of Pervasive Computing, Department of Computer Science and Technology, Tsinghua University, Beijing 100084, China. E-mail: liuyongjin@tsinghua.edu.cn.
- Y. He is with the School of Computer Engineering, Nanyang Technological University, Singapore 639798. E-mail: yhe@ntu.edu.sg.

Manuscript received 30 Dec. 2018; revised 2 Aug. 2019; accepted 28 Aug. 2019. Date of publication 5 Sept. 2019; date of current version 28 Jan. 2021.

(Corresponding authors: Minjing Yu and Yong-Jin Liu.)

Recommended for acceptance by T. Ju.

Digital Object Identifier no. 10.1109/TVCG.2019.2938746.



Fig. 1. Automatic pose generation in typical living and bedrooms.

Our main contributions are twofold:

- We develop a virtual tool to predict the fit between humans' anthropometric characteristics and the functionality of chairs, which enables ergonomic rating, exploration, and design improvement of chair models for individuals; and
- Using the generated sitting poses, we develop a metric to quantitatively measure the sitting position, pressure distribution and support area, and provide an ergonomic rating for chairs.

## 2 RELATED WORK

A large body of literature on human poses and man-made object analysis is available. Given that this paper focuses on the ergonomic rating of 3D chair models driven by the pose deformation of users' avatars, we review the most relevant work on virtual fitting, functionality representation of shape, ergonomic analysis and pose synthesis.

### 2.1 Virtual Fitting

In computer graphics, there are keen interests in simulating and visualizing the interaction between humans and object(s). Virtual fitting is a computational tool that aligns the virtual human body to fit the object/environment and then allows the users to check the visual appearance and evaluate the functional properties [1], [2], [3]. Towards this goal, dealing with geometry (e.g., the shapes of objects of interest and/or the poses of the human body) and physical constraints (e.g., collision and balance) is usually required. There are many works on virtual cloth fitting that investigates the interactions between wearers and clothing, such as collision detection [3], [4], cloth transfer and retargeting [5], [6], [7], and realistic clothing animation [8], [9], [10]. Other studies have also provided virtual try-on tools for customized shoes [11], eyeglasses [12], and Hijab fitting [13]. However, little work has been done for other objects in our daily lives.

In virtual fitting, the geometry of the user's body plays an important role to evaluate the fit status. Digital human model (DHM) has been widely used to replace expensive mockups due to its low cost and morphable characteristics. DHM data can be obtained from various ways, such as images [5], [6], [8], parameterization based synthesized models [1], [9], [10], or mannequin models [14]. The present study uses the 3D geometric avatar of the users reconstructed from an RGB-D camera [15], [16], thereby having irreplaceable superiority in fitting evaluation. We leverage the users' avatars to implement the virtual fitting of chair models, which enables the ergonomic assessment

and design customization of chairs to be realized with practical significance.

### 2.2 Functionality Based Shape Representation

The ergonomic assessment of furniture models, such as chairs, largely depends on the functional analysis of human poses and furniture, which has attracted increasing attention recently (e.g., [17]). We refer the readers to [18] for a comprehensive survey on evaluating functionality and affordance with humanoid agents.

Kim et al. [19] proposed an efficient method that can be used for fitting agents' poses. Another representative method proposed by Hu et al. [20] can recognize the functionality of objects by considering its interaction with its surroundings. The methods proposed in [19] and [20] are general approaches for pose generation, while our method focuses on a specific application in ergonomic ratings without the assistance of data sets.

### 2.3 Ergonomic Analysis

From the perspective of human factors and ergonomics [21], [22], all products designed for people aim to suit the human body and mind, make them feel safe and satisfied, and even provide enjoyment. Ergonomic analysis allows the engineers to analyze and score human comfort, safety and performance for targeted populations in the context of a designed product or workplace. Human factors and ergonomics are concerned with the fitting between the users and the products, which is affected by the geometrical and biological characteristics of the human body.

Ergonomic analysis methods mainly include heuristic and analytical evaluations [23]. Heuristic evaluation is conducted through identifying a checklist of conventional ergonomics issues. For office furniture and chairs' selection, their dimensional relationships with anthropometric variables have been investigated, and the ergonomic principles and checklists have been determined [24], [25]. Analytical evaluation enables users to evaluate the products or workplaces with respect to one or more of the physical loads, such as posture and forces. Posture-based and biomechanics-based analyses or even their combinations are developed to virtually screen harmful postures and simulate the loading in actions such as pushing, pulling, carrying, lowering, or lifting [26], [27].

Zheng et al. [28] proposed an ergonomics-inspired reshaping method that can evaluate the fitness of a given human skeleton pose and an object model. However, by using only a skeleton, one cannot consider the ergonomic rules related to pressure and support. In this paper, by employing a detailed human avatar model, we show that all of these ergonomic guidelines can be evaluated virtually and provide a better predication of chair fitness.

In our work, benefiting from the virtual fitting of a human avatar, we assess the ergonomic fitting of chair models in relation to fitness, pressure, and support. The rating is based on a checklist of the shape features of chairs that determines the sitting position. The ratings of pressure and support are considered by leveraging the surface deformation of chairs, which is caused by the users' weight and a specific pressure peak.

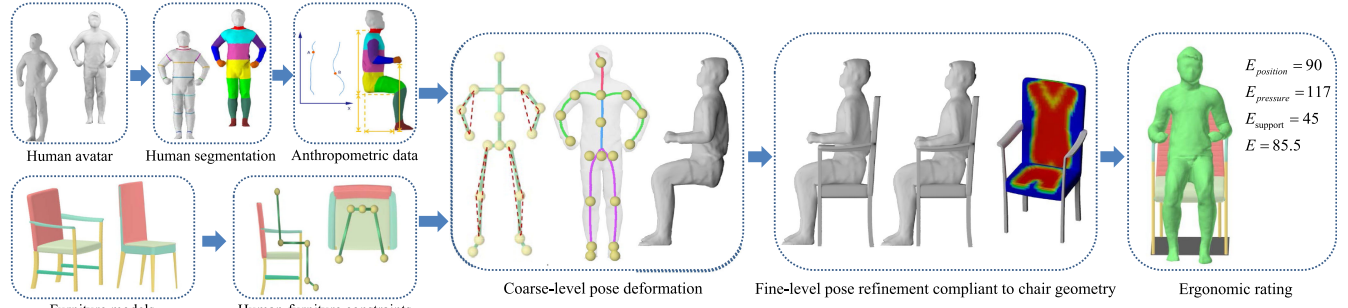


Fig. 2. Pipeline of our approach.

#### 2.4 Pose Synthesis

Deforming the skin of human to produce new poses is commonly involved in the animation generation and has attracted much attention in computer graphics. The main technologies can be classified into skeleton-based and example-based deformations. The skeleton-based deformation—also named as skeleton subspace deformation (SSD)—attaches an underlying skeleton to human meshes to perform skin deformation. It is the most popular method characterized by its simplicity and smooth results, which is computationally effective and widely used for real-time implementation [29], [30], [31]. By considering the interaction with the environment, Lin et al. [32] propose another representative work that creates sitting poses from user sketched skeletons. The example-based deformation—also called shape interpolation or shape blending—is a data-driven approach [33], [34], which models the deformation as a linear combination of a set of sample poses. However, it is rarely used in real-time application and cannot guarantee geometric continuity. As our method is concerned with the computation efficiency, we adopt the skeleton-based skinning to realize the automatic pose deformation for chair fitting.

In SSD, the linear blending skinning, initially proposed in [35], is the first direct skinning model for skeleton-based deformation. It is easy and intuitive to use, but usually has artifacts caused by volume loss for large deformations, such as elbow collapse and candy-wrapper twists. Many works about non-linear blending skinning have been reported to preserve the volume, such as log-matrix skinning (LMS) [29], spherical blend skinning (SBS) [30], and dual quaternion blend skinning (DQS) [31]. A joint bulging artifact could be further caused in DQS as DQS interpolates rotations around the same center of rotation at the joints [36].

Alternative attempts emerge to address the defects of SSD, such as combining SSD and shape interpolation [33]. Such combination is done using multidimensional weights per matrix to allow input transformations to be decomposed and blended separately [37], [38], and mapping the primary skeleton pose to the transformation of added helper bones [39]. However, these methods tightly rely on the stored pose examples and require heavy computational costs.

Our method utilizes a skeleton-based deformation method proposed by Le and Hodgins [40], which can avoid all the aforementioned artifacts by pre-computing the optimized center of rotation for all vertices from the rest pose and skinning weights. Our method only needs one input mesh and then binds the skeleton with the skin in a direct and geometrical way, which efficiently rigs the character for new poses.

### 3 OVERVIEW

The inputs of our approach are segmented chairs and human avatars. In our application scenario, chair products in online stores are always segmented with semantic labels. Since the human avatar is easy and affordable to obtain, our approach uses real human shape for sitting pose generation and ergonomic rating. The user study in Section 6 shows that using a real human shape helps achieve a good ergonomic rating.

Our method assumes that the 3D chairs are segmented with semantic labels. For unsegmented chair models, one can apply the existing methods of co-analysis and region annotation [41], [42]. Since our approach targets on ergonomic rating, we present a simple method in Section 4 to segment human avatars (acquired in a controlled environment where users make common poses such as standing) and represent them with assembled skeletons and skin meshes. Then we automatically align the specific human part with the corresponding chair part by considering the constraints of human-to-chair interactions. We propose a four-step algorithm to implement this alignment of the chair model and human models. In Section 5, we evaluate the ergonomic performance of chair models in terms of geometrical fit, pressure distribution, and contact area, and compute a rating of chair models. Section 6 presents that our method is scalable to other furniture, such as desks, beds, and cabinets. Fig. 2 shows the pipeline of our approach.

### 4 AVATAR REPRESENTATION AND DEFORMATION

In ergonomic analysis, a user's avatar is useful for integrating the user into the virtual environment for simulating the interactions between the user and the workplaces or products. The avatar, which is the geometrical representation of the real human body, enables the engineers to consider ergonomic and human factor during the product development. Furthermore, the avatar makes the validation of the ergonomic functions of the products (without the need of real experiments) possible, which speeds up the production and trade process. The 3D avatars can be quickly reconstructed on the basis of existing work [15], [16].

To measure the anthropometric data and deform the avatar to fit ergonomic constraints, we segment the human body into different body parts and represent each avatar by a skin mesh with an assembled skeleton (Section 4.1). The deformation of skin mesh is then driven by the deformation of the skeleton (Section 4.2).

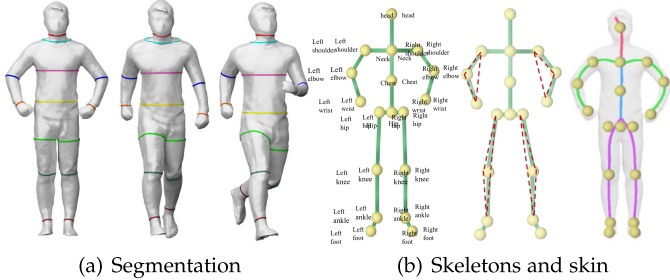


Fig. 3. Avatar segmentation and representation by a skin mesh assembled with a skeleton.

#### 4.1 Pose-Free Segmentation

The curved skeleton of the avatar is extracted by the thinning algorithm [43]. The shape of the human body is then cut into slices at every skeleton point. Each slice corresponds to the contour of a cross-section perpendicular to the curved skeleton. To determine the segmentation position, we compute a set of properties for each slice, including the center of the slice, average radius, average curvature and intersection angle. On the basis of these properties, we determine the segmentation lines on the head and limbs by the geometrical definitions specified in Appendix (Section A2), which can be found on the Computer Society Digital Library at <http://doi.ieeecomputersociety.org/10.1109/TCVG.2019.2938746>.

After segmenting the head and limbs from the human body, the trunk is segmented according to the contours of the laterals. In more details, we sort all the slices on the trunk by arranging them according to their height in descending order, and then project the points on these slices to the 2D plane to generate the contour of the trunk. Subsequently, we traverse the front and back contours of the trunk to determine the segmentation positions. On the front contour, the concave point having the smallest intersection angle is considered the segmentation position for the junction of the chest and waist. On the back contour, the point having the smallest intersection angle is regarded as the segmentation position for the junction of the hip and waist. The slices consisting of these segmentation points are taken as the segmentation lines. Given that the curved skeleton is generated from the human body without a specified pose, the segmentation is able to deal with the avatar with various poses (Fig. 3a).

#### 4.2 Skinning Model and Deformation

The avatar generally needs to deform the body shape and acquire a new pose to match with the chair models during virtual fitting. Presently, the skeleton-based deformation technique is still the most efficient way of rigging the character into new poses by only inputting the mesh model. Considering its advantages in terms of computational cost and without the need of pose samples, we adopt the skeleton-based technique for pose deformation.

Expanded from Chen et al.'s work [44], we use an 18-joint skeleton model to describe the human's pose (Fig. 3b left). The skeleton nodes of a given human body can be automatically generated by locating the nodes on the curved skeleton extracted from shape segmentation, which saves the step of skeleton embedding into the human body.

Thereafter, the skeleton model is constructed by a tree structure consisting of a set of node joints connected by the edges (also called bones). The hip joint is set as the root of the tree and denotes the origin coordinate of the world coordinate with  $x$ ,  $y$ , and  $z$  axes. When a pose of the human model is deformed to another one, it needs to align them in the same world coordinate and then align the joint coordinates. As each joint within this skeleton is possibly active with three DOFs and may lead to arbitrary poses, we add additional constraints on the pose description to consider the human's biological limitation: (1) the elbow cannot rotate to the shoulder or the wrist, (2) the skeleton of the real human body is not scalable or stretchable; thus, the 17 edges in the skeleton model are fixed in length and can only be rotated, and (3) the knee and elbow joints belong to hinge joints and only permit motion in a plane. Thus we define four triangle planes for the left and right elbows, and left and right knee joints (Fig. 3b middle).

With the assembled skeleton and skin meshes, skinning is the process to bind them and enable the deformation of the skin meshes to follow the deformation of the skeleton. To avoid the artifacts of elbow collapse and candy-wrapper twists, we use the skeletal skinning method with optimized centers of rotation in [40]. Briefly speaking, given a meshed human body with an embedded skeleton and vertices weights, let  $T_j$  ( $\forall j = 0, \dots, k$ ) be the transformation matrix of bones  $B = (b_0, \dots, b_k)$  with weights  $W = (w_0, \dots, w_k)$ , which includes the rotation matrix  $R_j$  and translation vector  $t_j$ . The transformation of each vertex  $v_i$  on the mesh can then be computed from  $T_j$  and  $W$ . As the bones of the human skeleton are not stretchable in our method, except for a global translation, the transformation of bones should not include any translations but only rotations. The computation of transformation is then updated as follows:

$$v_i' = \sum_{j=1}^m w_{ij} (q_j(v_i - p_j) + p_j'), \quad (1)$$

where  $p_j$  is the original position of bone  $b_j$  and the center of rotation,  $p_j'$  is the updated position of  $p_j$  in the new pose, and  $q_j$  is unit quaternion that is converted by the multiplicative rotation matrixes  $R_j \cdots R_k$  of bone  $b_j$  and all its ancestors.  $p_j$  can be substituted by the optimized center of rotation  $CoR_i$ ; see [40] for details.

## 5 ERGONOMIC EVALUATION OF CHAIRS

In ergonomically designing chairs [45], the general principle is that the chair should fit the user according to his/her own shape and provide a comfortable feeling by providing sufficient support to the human body in the sitting posture. Therefore, the ergonomic rules are mainly related to the contact boundaries between the user and chair during sitting, i.e., the back, arms, buttocks and thighs, popliteal area, and feet (Fig. 4). Ergonomic rules can also be described through the geometric structure and contact constraints using quantitative terms including the chair design parameters, user's anthropometry, the pressure felt by the user, and the comfortable support provided by the chair [24], [25], [45]. Traditionally, these terms (in particular the last two) are evaluated on the basis of the subjective assessment

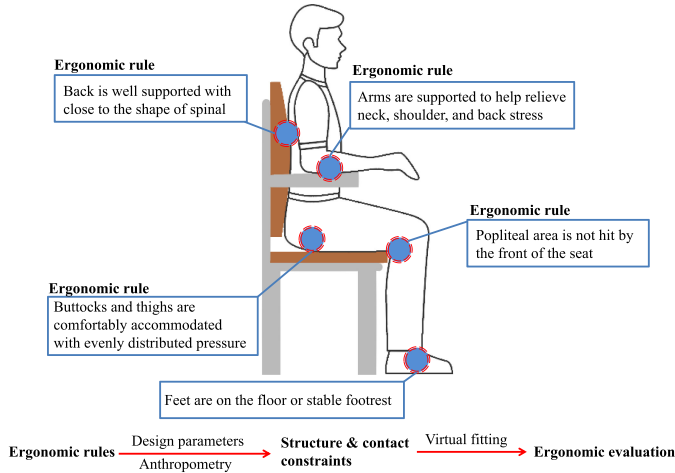


Fig. 4. Ergonomic design and evaluation of chairs.

of several participants. However, this endeavor is costly and time-consuming to carry out.

By providing the segmented chair, our method can automatically measure the chair design parameter (Section 5.1). In Section 5.2, we present a virtual fitting method that aligns the human body and chair model. The primary advantage of this method is that it can provide an efficient and accurate anthropometric data of the avatar in sitting pose; together with the deformation of chair contact surface (Section 5.3), the method can further provide the pressure distribution and support intensity for ergonomic ratings (Section 5.4).

## 5.1 Design Parameters

During the furniture design process, a list of design parameters is required to define the product's structural organization and functional characteristics and to accommodate the dimensions of the human body ergonomically. For chairs, seat-pan and backrest are the most important support for users. Fig. 5 shows the seven main ergonomically-guided design parameters [46], which are listed as follows.

*Seat-pan height*  $h_s$  is the distance of the foremost surface point of the seat-pan from the floor. An appropriate seat-pan height allows the user's thigh to be in a horizontal position and the feet to be supported by the floor. It is also aligned with the popliteal height of the user, ensuring the pressure on the buttocks and thighs to be distributed evenly while sitting.

*Seat-pan width*  $l_{sw}$  is the maximum horizontal length of the seat-pan. For chairs with armrests, seat width is the distance between the left and right armrests. The width should ensure the buttocks to be fully supported and should enable appropriate relaxation. Specifically, the width of chairs with armrests should be based on the width of the user's shoulders so that the arm of the user can be freely placed on the armrest.

*Seat-pan depth*  $l_{sd}$  is the maximum vertical length of the seat-pan. The seat-pan depth should be able to approximately cover the length of the user's thigh. A seat-pan that is too deep will lead to a great incline when the user leans against the backrest and a lack of support for the waist muscles, whereas a seat-pan that is too shallow will cause knee numbness due to overpressure on the knees.

*Seat-pan angle*  $\theta_s$  is the angle between the seat-pan surface and the horizontal plane, which measures the degree of inclination of the seat-pan.

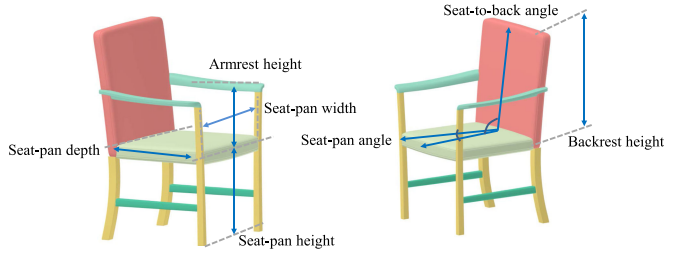


Fig. 5. Design parameters of chair.

*Seat-to-back angle*  $\theta_b$  measures the degree to which the backrest reclines, which is formed by the backrest and seat-pan. A backrest angle close to the human's shape of spinal column could prevent sliding forward and retreating pelvis.

*Backrest height*  $h_b$  includes the height from the top point of the backrest to the point of lumbar support and the height from the lowest point of the backrest to the point of lumbar support. The curved shape of the waist should be supported to keep the balance of the spinal column.

*Armrest height*  $h_r$  is the vertical distance from the seat-pan to the top of the armrest. It should be comparable with the user's elbow height. A high armrest makes shoulders hunched up, whereas a low armrest may not provide support for the arms at all.

## 5.2 Constraint-Based Sitting Pose Generation

Given the segmented human avatar, we generate a sitting pose by deforming and aligning the human body to the chair model. To have a good alignment, we consider the chair's geometry and its contact with the human body. Our algorithm takes chairs with semantic labels as input, and computes the above-mentioned design parameters, which are used to set up the geometrical structure constraints and to generate an initial fitting pose. The geometrical constraints lay the basis to deform the human body with an initial fitting pose on the coarse level. We then consider the contact-preserving constraints that provide comfort through contacting support for the human body during usage and can be used for the body-chair alignment on the fine level. We list the geometrical structure and contact-preserving constraints in Appendix A3, available in the online supplemental material and refer the readers to [47] for the ergonomic design guideline. Furthermore, we consider the self-collisions on the human body and collisions between the human body and chair, which are specified in Eq. (4).

With the prescribed constraints, we design the human-to-chair fitting alignment using a two-level process: a coarse-level pose deformation and a fine-level pose refinement. At the coarse level, we first deform the human into an initial fitting pose according to the geometric structure of the chair. Then, we further refine the pose part-by-part at the fine level according to the contact constraints. As different body parts in practice usually undertake different biological functions during chair usage (e.g., the buttock acts as the root of the skeleton and barycenter of body, while the limbs offer substantial support for the body through interactive contact outside), we successively refine the human's pose aligned with the chair model by the order of hip, trunk, and limbs. In total, there are the following four steps to realize the coarse- and fine-level pose deformation for human-to-chair fitting alignment.

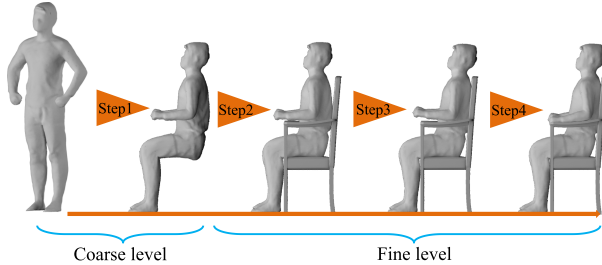


Fig. 6. Four-step alignment of the shape of the human body and the chair model. See text for details.

**Step 1 Pose Initialization.** In the process of virtual fitting, an initial fitting pose of the human body is generated at the coarse level according to the geometrical structure constraints. In the case of the chair model, the upper and lower limbs are set as being hanged down vertically, and the joint angles of elbow and knee are set at 90 degrees. The joint of human's hip  $J_{hip}$  is set as the rotation center; the quaternion for rotation is computed by the transformation vector, which is originally obtained by  $p_{knee} - J_{hip}$  ( $p_{knee}$  is the feature point of interior knee) and is transformed by increasing its  $y$  coordinates with knee height  $h_{knee}$  and seat-pan height  $h_s$  by  $\|h_{knee} - h_s\|$ . Then the quaternion can be used to rotate the thigh bones and lift the thighs and legs. The seat-pan height of the chair model determines the placement of knees, that is, the thighs should be parallel to the seat-pan under the condition  $h_{knee} \leq h_s$ . Otherwise, the thighs and legs are elevated to enable the feet to be placed on the floor. For the angle between thighs, we set  $\theta_{thigh} = 30$  degrees when there is no armrest or the seat-pan width  $l_{sd}$  is wide enough; otherwise,  $\theta_{thigh}$  is decreased until the knee width  $l_{knee}$  equals to the seat-pan's width.

**Step 2 Body Translation.** With the initial fitting posture, this step starts to finely align the human body with the chair model through contact-preserving constraints. First, we move the human model to attach to the chair. Given that the buttocks usually act as the barycenter of the human body, we compute the pairs of contact points on the buttocks ( $p_{contact}$ ) and on the chair component ( $p'_{contact}$ ) by the optimization solver for Eq. (2), and then achieve the translation of the human body led by the translation of  $p_{contact}$  to  $p'_{contact}$ . For the chair, the contact constraint occurs between the buttocks and the seat-pan, and the human body will be attached to the chair by translation to the contact points on the seat-pan.

**Step 3 Torso Transformation.** If there is contact constraint for the trunk, then this step further deforms the pose by the transformation of the trunk. The optimization solver is used to compute the contact point pairs and vector  $p_{contact} - p'_{contact}$  and then achieve the deformation. Specific chair may consist of a non-straight backrest to support the trunk. We can treat the trunk as two parts connected by the chest-hip bone and the chest-neck bone, and then individually perform the transformation of the two pieces with the optimization solver.

**Step 4 Limb Transformation.** The limbs of the human skeleton are the upper arm, forearm, hand, thigh, leg, and feet. As the end effector in inverse kinematics, hands and feet are dealt with contact constraints. If the hands or feet have contact interaction with the chair model, their transformations are obtained via the optimization solver. If a hand touches

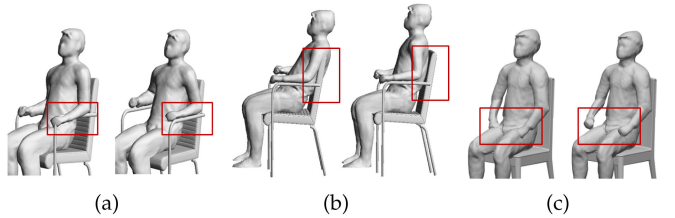


Fig. 7. Two types of collision: human-chair collision (a,b) and human self-collision (c).

the body, such as a thigh in a sitting posture, then the optimization solver can be applied to search for the contact points and perform transformation. In most cases, the feet contact is the floor, and only foot movement with its adjacent parts is needed through the skeletal hierarchy. The forearm, upper arm, leg, and thigh accordingly finish transformation according to possible contact constraints.

Fig. 6 demonstrates the pose deformation through the 4-step alignment in the case of virtual fitting on a chair model. At the coarse level, an initial sitting pose is generated in step 1 according to the geometrical structure of the chair and then steps 2-4 refine the pose to tightly match with the chair through human body translation, trunk and limbs transformation at the fine level.

The 4-step alignment is realized by minimizing the following objective function:

$$\varepsilon = \varepsilon_{contact} + \varepsilon_{collision} + \varepsilon_{joint}, \quad (2)$$

which considers the biological limitation of humans, described by the freedom degree of skeleton joints  $\varepsilon_{joint}$ .

Contact term  $\varepsilon_{contact}$  measures the corresponding compartments of the human body and chair with contact relations as specified below. We compute the set of contact points on deformed human meshes, which have the closest euclidean distance with the chair, and define  $\varepsilon_{contact}$  as

$$\varepsilon_{contact} = \sum_i (q_i(u, \theta)(p_i - x) + x'(u, \theta) - a_i)^2, \quad (3)$$

where  $(u, \theta)$  is the rotation axis and angle of the quaternion,  $q_i$ ,  $p_i$  is the contact candidate point<sup>1</sup> on the human mesh,  $x$  is the rotation joint of the corresponding bone of  $p_i$ ,  $x'$  is the updated position of  $x$  in the deformed pose,  $a_i$  is the closest point on the chair compartment to  $p_i$ .

Collision term  $\varepsilon_{collision}$  is to handle possible collision in the pose deformation. During the contacting process, the human body may generate self-collision between limbs (e.g., the hand penetrates the thigh) or the human body may generate collision with the chair model (e.g., the hand penetrates the armrest or the back penetrates the backrest); see Fig. 7 for examples. We define the collision term similar to [32]:

$$\varepsilon_{collision} = \sum (\|v_1^k - v_2^k\| - \|v_1^{k-1} - v_2^{k-1}\|)^2, \quad (4)$$

where (a) in limb-limb collision,  $v_1$  and  $v_2$  are the two points on the bones of two limbs closest to the collision point, and

1. Contact candidate points are determined as a selected part of the human body whose initial positions are within a small distance threshold between the corresponding body and chair parts.

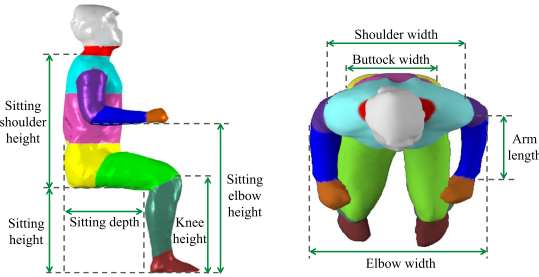


Fig. 8. Anthropometric variables of a sitting avatar.

(b) in human-chair collision,  $v_1$  is the collision point and  $v_2$  is the point on the bone closest to the collision point.

Joint term  $\varepsilon_{joint}$  is to keep the pose deformation in a physically feasible range through the joints of skeletal structures. Referring to [48], the joint limit constraints can be enforced by controlling the relative orientation between two adjacent bones; that is, when the joint angle between the two adjacent bones exceeds the prescribed limit,  $\varepsilon_{joint}$  is added into the minimization process during iteration. Thereafter,  $\varepsilon_{joint}$  is designed as follows:

$$\varepsilon_{joint} = \sum_{i,j} \{[q_i(u, \theta)v_i - q_j(u, \theta)v_j] - v_{max}\}^2, \quad (5)$$

where  $v_i$  and  $v_j$  are the vectors of two adjacent bones after transformation and  $v_{max}$  is the target vector between them with correct limit angle. To improve the performance of computing the above equation, we use the vector difference of two bones instead of directly using the angle to define the constraint.

We adopt the hill climbing algorithm [49] to solve the optimization problem in Eq. (2), which is fast and easy to implement. The solver takes the body parts and chair components as input, and computes the deformed body parts after rotation transformation. During each iteration, when collision or joint angle violation is detected, the collision term  $\varepsilon_{collision}$  or joint limit term  $\varepsilon_{joint}$  will be added into global energy term  $\epsilon$ , and the solution in such an iteration will be recomputed again until no collision or joint angle violation occurs. Since  $\varepsilon_{contact}$  is strictly decreasing in each iteration,<sup>2</sup> the hill climbing algorithm is guaranteed to converge.

By virtual fitting with realistic human body geometry, the anthropometric data of a segmented avatar in the sitting posture (Fig. 8), including the sitting height, sitting depth, elbow height and width, arm length, are readily obtained.

### 5.3 Deforming Contact Surface

Given the pressure force from the human body during the contact process, we need to model the surface deformation of the chair model to reflect the mechanical performance of the chair material and ergonomically rate the pressure and support factors (Section 5.4).

We voxelize the chair model and use the spring-mass system to simulate the surface deformation of the chair model. The center of a voxel represents a mass node in the mass-spring system and is denoted as  $m_i$ ,  $i = 1, \dots, n$ . During the deformation process, each mass is possibly exerted by three

2. Here we exclude those iterations to be recomputed.

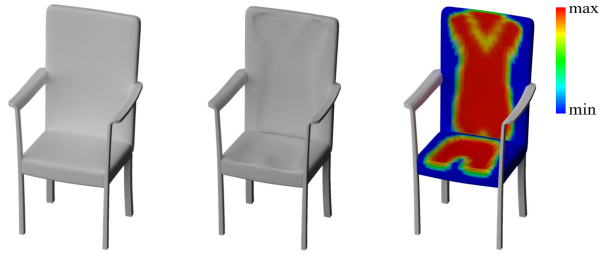


Fig. 9. Deformed surface and pressure distribution of a chair model during sitting.

types of forces: spring, damping, and external forces. Here, we concern the pressure force as the external force for each mass. All the mass nodes that are within the distance of 10 mm from the sitter's skin are chosen to be the receptor for the pressure force during the sitting contact time. The pressure force on the seat-pan is computed by  $F_i^e = \frac{G_{hb}}{A_{touch}}$ , where  $G_{hb}$  is the gravity of the human body,  $A_{touch}$  is the contact area and is accounted as the number of mass nodes. The pressure force on the seatback is computed by  $k_e F_i^e \cos \theta_b$ , where  $k_e$  is a constant and  $\theta_b$  is the angle between the seat-pan and seatback. The damping force is dependent on the velocity of  $m_i$  and is computed by  $F_i^d = -dv_i$ , where  $d$  is the damping coefficient. The spring force is generated when the length of the spring between two mass nodes is changed, which is computed by Hooke's law:

$$F^s(m_i, m_j) = K(L_0 - \|m_i - m_j\|) \frac{m_i - m_j}{\|m_i - m_j\|}, \quad (6)$$

where  $L_0$  is the initial length of the spring, and  $K$  is the elasticity coefficient that is determined by the mechanical functions of the chair material within a typical range [0.1, 10] Gpa. With the input of the pressure force, we are able to compute the force and motion velocity of each mass node with increasing time steps until the mass-spring system reaches the steady state. We use the midpoint method instead of the Euler method to solve the dynamic equations for the purpose of a more accurate solution.

After computing the voxel displacements, we deform the chair model by updating its vertex coordinates accordingly. The movement of a triangle of the chair is the average displacement of all the voxels that have an intersection with this triangle, and the movement of each vertex is the average movement of all its adjacent triangles. Fig. 9 shows the deformation of the surface and pressure distribution of a chair model after sitting contact.

We iteratively alternate the computation of chair contact surface deformation and fine-level sitting pose generation, until both the contact surface and the pose remain unchanged. In our experiment, two iterations are usually enough.

### 5.4 Ergonomic Rating

Compared with subjective measurement by employing subjects through questionnaires, the ergonomic rating is a fast and effective way to evaluate whether the functions of the chair models meet the ergonomic requirements of a specific user. The ergonomic characteristics of the chair model are measured in terms of the user retaining a comfortable sitting

position, good pressure spread, and strong support [45]. Thus, we develop an objective comfortableness metric  $E$  to rate the ergonomic performance of the chair model with three terms:

$$E = w_0 E_{position} + w_1 E_{pressure} + w_2 E_{support} \quad (7)$$

$E_{position}$  is the rating score about the shape and size of the chair model fitting to the sitter's dimensions. The rating is based on the ergonomic guidelines for the chair in terms of a checklist of the most universal shape features [25], which are derived from people with considerable experience. In practice, there are separate checklists of ergonomic issues for each type of furniture or equipment, which can be used for evaluation accordingly. We calculate the rating score of  $E_{position}$  in the chair case by taking the sum of the scores of each ergonomic issue  $I_i$  in the checklist (as listed in Table A1 in the Appendix, available in the online supplemental material), i.e.,  $E_{position} = \sum_{i=1}^m I_i$ . For each  $I_i$ , by concerning the shape matching extent between the human and chair models, the extent is mapped to one of the three scores (20, 10, and -10) depending on their values.

$E_{pressure}$  is the rating score for pressure distribution at the interface between chair and sitter. Pressure distribution is the most frequent investigation of the feel characteristic of the chair, which is more complex in the biological mechanism and receives recent attention [50]. We calculate the proportional pressure and pressure gradient on the contact surface to quantitatively represent the pressure distribution term, e.g., a soft seat cushion will form a pressure gradient with a gradual decrease toward the front and sides, while the hard seat-pan without a cushion will have no pressure gradient and the sitter is not comfortable. The pressure gradient is concerned with the displacement gradient of mass nodes on the surface voxels in the spring-mass system at the steady state. Let  $v_i$  and  $g_i$  be the displacement and displacement gradient of each surface voxel, respectively. We compute  $E_{pressure} = 100(P_c + \Delta P)$ , where  $P_c = \frac{\sum_{i=1}^n v_i}{\max_i \{g_i\}}$  measures the pressure magnitude, and  $\Delta P = \sum g_i$  measures the pressure gradient.

$E_{support}$  is the rating score of the support intensity of the chair model to the sitter, which is mainly influenced by the contour of the chair and the posture of the sitter. A substantial association exists among the support parameter, the fit, and pressure parameters. We calculate it by computing the contact area between the user and the chair considering the user is sitting with a standard constrained posture rather than with an arbitrary posture. In our method, the contact surface is computed by the summed area of the number of voxels which have contact with the body surface, thus  $E_{support} = 100 \frac{nL_v^2}{S_{back} + S_{buttock} + S_{thigh}}$ , where  $L_v$  is the voxel length, and  $S_{back}$ ,  $S_{buttock}$  and  $S_{thigh}$  are the voxel area of the surfaces of the back, buttock and thighs.

## 6 EXPERIMENTAL RESULTS

We implement the proposed algorithm in C++ and test it on a PC with i5-6400 2.7 GHz CPU and 8G RAM. Source codes will be publicly available. Our algorithm is efficient, and it takes less than 10 seconds to generate a sitting pose. For the ergonomic metric (ref. Eq. (7)), we set  $w_0 = 0.5$ ,  $w_1 = 0.25$  and  $w_2 = 0.25$  in all our experiments.

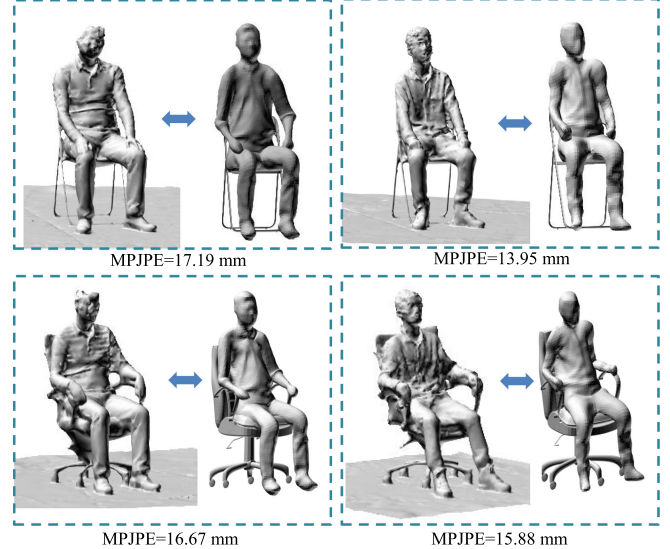


Fig. 10. Similarity evaluation between the ground truth (left) and virtual fitting results (right).

Our method allows users to dress in loungewear so that the scanning for human avatar is flexible and virtual try-on can better match users' daily life experience. Section 6.1 reports the accuracy of virtual fitting and Section 6.2 presents a user study to show the effectiveness and efficiency of our method. Sections 6.3, 6.4, 6.5 present more results on different application scenarios, method extension, comparison and discusses the merits and limitations of our method.

### 6.1 Virtual Fitting Accuracy

We conduct a preliminary study on the accuracy of virtual fitting in our method. We used FARO Focus3D X330 scanner (distance accuracy  $\pm 2$  mm and scan range (0.6m, 130m)) to scan the human avatars of two users, two selected chairs, and their sitting poses on these two chairs. Then we manually segment the scanned chair models. To evaluate the accuracy of our method, then we compare the scanned sitting pose results (as the ground truth) with the generated sitting pose results obtained by applying our method to the human avatars and scanned chairs (Fig. 10).

To measure the similarity between the ground truth and our method, we follow [51] to use the metric of the mean per joint position error (MPJPE), which is the mean of errors of all joints between the scanned and deformed humans skeletons

$$E_{MPJPE}(S) = \frac{1}{N_S} \sum_{i=1}^{N_S} \|m_S(i) - m_{S'}(i)\|_2 \quad (8)$$

where  $N_S$  is the number of joints in skeleton  $S$ ,  $m_S(i)$  is the predicted coordinate of  $i$ th joint, and  $m_{S'}(i)$  is the coordinate of  $i$ th joint in the ground truth. As shown in Fig. 10, the MPJPE values of our method in all the four sitting poses are less than 20 mm. Our results are much smaller than the best results (that are more than 110 mm) in [51]. The measured error range (10 mm, 20 mm) in our method also fits the allowable error range (< 100 mm) in anthropometric measurements for clothed participants for office furniture design (Table 1, page 7 in [47]).



Fig. 11. Top row: thirteen chairs in a furniture chain store are used in our user study. Bottom row: these chair models are scanned with manual segmentation.

## 6.2 User Study

We recruited  $n = 10$  participants, eight males and two females, with ages ranging from 20 to 38. Among them, there are two overweight and two underweight. We conducted our user study at a furniture chain store with 13 types of chairs (see Fig. 11). We asked each participant to try the chairs and give a ranking to 13 chairs as the ground truth. In more detail, participants provided their rating scores in the range [0, 100], with a reference to the interval scales of “excellent” (80-100), “good” (60-80), “fair” (40-60), “poor” (20-40) and “bad” (0-20), which is a variant of the ITU-R five-point quality scale [52]. We collected the rating scores of participants in two steps. In the first step, the participants tried each chair and wrote an initial score for it. In the second step, the participants modified their scores by trying each chair one more time. This two-step procedure ensured that the score for each chair was given based on the feeling of trying *all* chairs. To eliminate the potential bias among different participants, we converted all the scores provided by a single participant into a ranking. We used the ranking data of all participants as the ground truth. To investigate the consistency of rankings by different participants, we performed a two-way ANOVA analysis and the p-value is 0.00187 (which is much less than the cutoff point 0.05), indicating significant correlation of rankings of different participants.

Our goal is to design an automatic ergonomic rating method that has a high agreement with human preference. Then we chose to compare our approach with two related representative methods: one is the traditional chair ergonomic rating method [24] (denoted as MT) and the other is an automatic rating method that uses a stick figure model instead of a real human model (denoted as MS). Both MT and MS methods can only perform the evaluation using the measured or estimated sitter’s anthropometry (ref. the scoring rules in Table A1 in the Appendix, available in the online supplemental material), i.e., they cannot make use of the terms on  $E_{pressure}$  and  $E_{support}$ . For MT, we measured the anthropometry data of the participants and manually compared them with the design parameters of the chair to evaluate the score according to the rules in Table A1 in Appendix, available in the online supplemental material. However, some anthropometry data, such as the sitting depth, sitting elbow height, can not be accurately measured due to the dress of loungewear. For MS, since the stick figure model has no body shape, we can only measure the lengths of bones to compare them with the design

parameters of the chair for the evaluation, which usually has less accuracy than MT.

We scanned the chairs and the body geometries of the participants. The scanned chair models were manually segmented and, from the scanned avatars, the skinning models with assembled skeletons were generated with pose-free segmentation (Section 4). Some real and virtual fitting results are shown in Fig. 12 and more results of all fittings on 13 chair models are illustrated in Appendix A5, available in the online supplemental material. We compute the scores of three methods (ours, MT and MS) for each pair  $(A_i, B_j)$ , where  $A_i$  is one of ten participants and  $B_j$  is one of thirteen chair models, and then convert these scores into rankings of chairs. To analyze the degree of similarity between two sets of ranks for the same objects, we adopt the Kendall independent test [53] to examine the consistency of the ranking by one of three methods with respect to the ground-truth ranking provided by the participants. Denote by  $\{x_i, y_i\}_{i=1}^n$  the set of observations of the continuous random variables  $X$  and  $Y$ . Any pair of observations  $(x_i, y_i)$  and  $(x_j, y_j)$ , where  $i < j$ , are said to be concordant if the ranks for both elements agree, i.e.,  $(x_i - x_j)(y_i - y_j) > 0$ , otherwise, they are said to be discordant. If  $x_i = x_j$  or  $y_i = y_j$ , then the pair is neither concordant nor discordant. The Kendall coefficient  $\tau$  is defined as

$$\tau = \frac{n_c - n_d}{n(n-1)/2},$$

where  $n_c$  and  $n_d$  are the number of concordant and discordant pairs respectively. The value of  $\tau$  is in the range of  $[-1, 1]$ , where 1 means a perfect agreement between the two rankings and -1 indicates the absolute disagreement between the two rankings. In the presented study, the  $\tau$  values of our method, MT and MS are 0.89, 0.75 and 0.63,



Fig. 12. Examples of real and virtual fitting on the chair models.

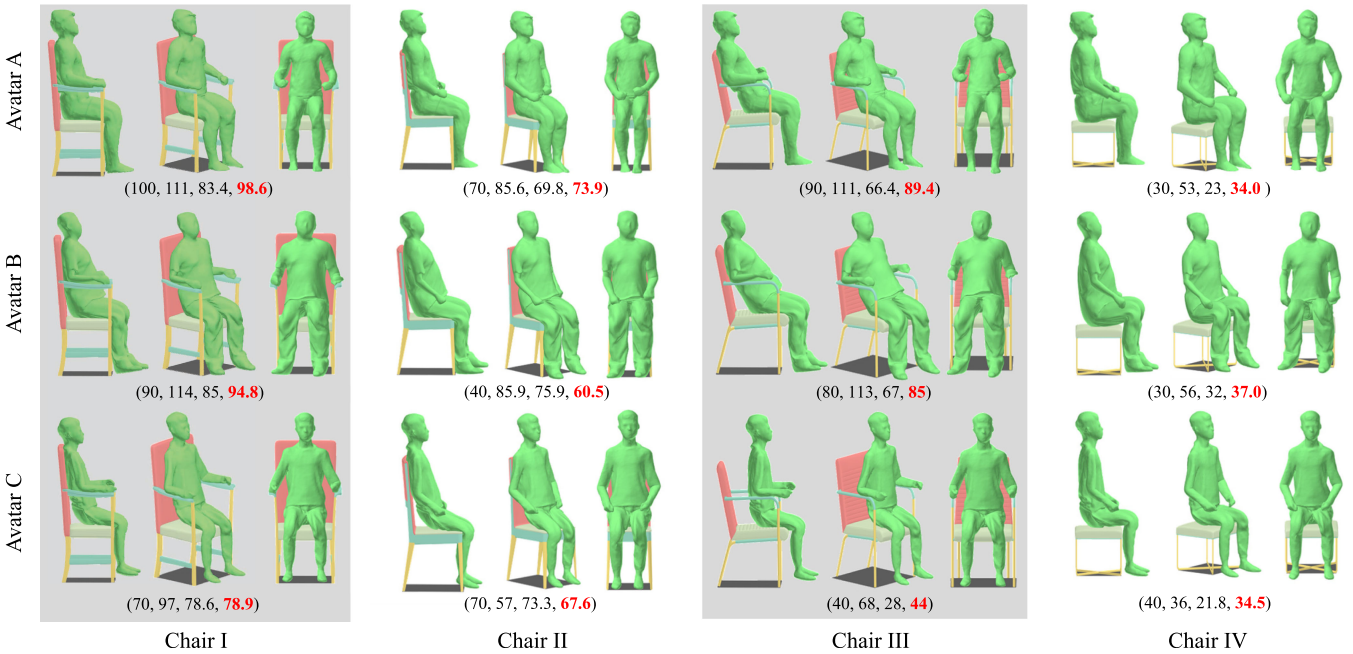


Fig. 13. Virtual fitting of four chair models by three avatars. The 4-tuple below each pair of (chair, avatar) is ergonomic ratings ( $E_{position}$ ,  $E_{pressure}$ ,  $E_{support}$ ,  $E$ ), in which the final metric value  $E$  is illustrated in red.

respectively, demonstrating that our method can provide the most accurate evaluation.

It is worth noting that we design a two-step process to collect rating scores of participants that ensures the equal importance of the ranking of every chair in the full list. Then we use the full ranking of thirteen chair models to evaluate how a ranking algorithm correlates well with human judgments. In practice, our evaluation metric in Eq. (7) can work with a top- $k$  query strategy [54] that is efficient for online store applications.

### 6.3 More Results

*Virtual Fitting.* Fitting the customers with the product is the best way to persuade the customers to make the decision to buy it, which is the reason why the merchandise vendors try their best to enable people to experience their products and service. Thus, with our approach, the vendor can demonstrate chair products oriented to different customers and check the fitting score of potential users. Once the avatars of the users are available, chair models can be virtually aligned and fitted with different avatars.

Fig. 13 illustrates the virtual fitting of four chair models with different shapes and styles by avatars A, B, and C with different dimensions. Chair model I has a different match to the three avatars that have different seating depths. Avatar A has close seating depth with the seat pan depth of the chair and thus has excellent support on the back part. Avatars B and C have shorter seating depths and need to be inclined to the backrest slightly. Furthermore, the seating height of avatar C is shorter than the seat pan height; thus, his feet cannot touch to the floor. All three avatars have support from the armrest with different elbow angles: B and C have a larger elbow angle than A. Chair II has no armrest but a narrow seat-pan width. Thus, the thigh angle of the sitter can be decreased to fit the thighs on the chair. The thigh angle of avatars A and B is narrower than that of

avatar C. Chair model III has a deep seat-pan depth. Avatars A and B have a seating depth of over 0.75 times the seat-pan depth so they can be inclined to contact with the backrest, whereas avatar C does not reach the contact condition of the backrest and keeps his back straight. Chair model IV is a bench with a short seat-pan height. Avatars A, B, and C can touch the ground and still need to elevate their knees. Fig. 13 exhibits the ergonomic scores of avatars A, B, and C on the four chair models. The chair products are easily accepted through the virtual fitting by the users who are most suitable and have the highest ergonomic score.

*Model Exploration.* Exploring the products and finding the most suitable one is usually the most time-consuming process for customers during shopping. Regarding the traditional way, customers spend time visiting different shops and trying various products personally to evaluate the best one. Concerning online shopping, people often continuously retrieve and evaluate the products depending on comparing the size specifications and judging by experience. Few alternatives are available to speed up this process especially for furniture products. Our method can offer an efficient way for a customer with the reconstructed geometrical avatar to explore chair models and quickly find out the most comfortable option through automatic virtual alignment and ergonomic ratings.

Fig. 14 presents the exploration results of a collection of ten chair models for avatars A, B, and C. Customers can easily compare the ergonomic scores of different chair models and find the best purchase via ergonomic rating results on the virtual fitting of the model. Furthermore, we can apply this method to a family to choose chair suitable for their home. For instance, in Fig. 15, a family can virtually fit the bench and sofa models, comparing the ergonomic scores for their sizes to make buying decisions.

*Design Optimization.* Optimizing the design for customization is to offer a desirable product for the customers, which is

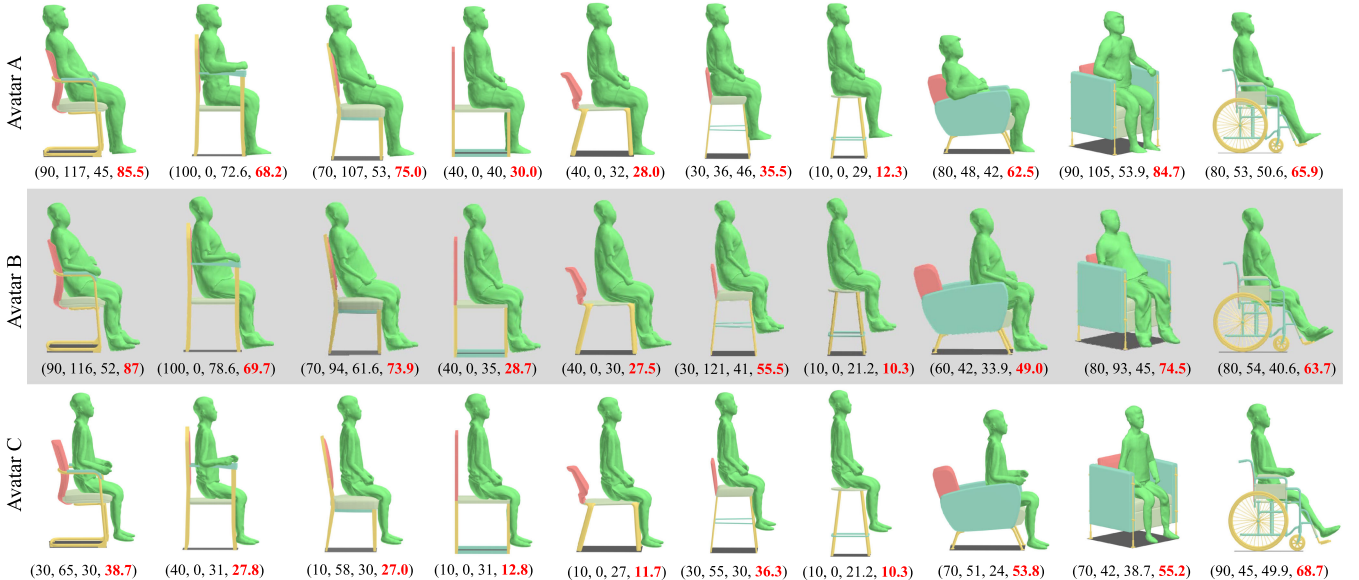


Fig. 14. Exploration results of a collection of chair models for three avatars. The 4-tuple is ergonomic ratings ( $E_{position}$ ,  $E_{pressure}$ ,  $E_{support}$ ,  $E$ ).

an essential step for manufacturers and designers during the design cycle. Although designers use personal statistical data in the design to accommodate the most significant of the population, furniture products still only provide 75 percent of target customers. Customized design is an efficient way to solve this problem and enhance the added values of furniture products. Our method endows benefits to the furniture designer to optimize the design for customization with the precise dimensional data of the avatar. The designer can traverse every index in the ranking score and optimize design parameters and material elasticity of the chair models to achieve a best ergonomic score with the ergonomic rating of a specific avatar in three terms ( $E_{position}$ ,  $E_{pressure}$  and  $E_{support}$  in Eq. (7)). Fig. 16 reveals several examples of chair models improvement by fitting a high ergonomic score and thus achieving high-quality customization.

#### 6.4 Extension

Although the above sections mainly focus on chairs, it is worth noting that our method can be extended to other types of furniture with given structure constraints and contact-

preserving constraints between human and furniture. Fig. 17 demonstrates our approach on chaise longue, office desk, and chair, bed, and cabinet. We determine constraints for each furniture model via the furniture model's geometric features and functionality. For the chaise longue, we borrow the chair's constraints and add contact constraint to characterize its leg support. For the study desk, the contact interaction usually occurs between the upper limb and tabletop; thus we are only concerned with limb transformation in the fitting alignment. Given the simple geometry of the bed (planar mattress), we can quickly generate the lying down pose with only the body translation. For the cabinet, the frequent interaction is to open/close the door via the handle, and we set the hand-on-the-handle constraint as the contact constraint. We list the structure constraints and contact-preserving constraints of the bed and cabinet models in Appendix A3, available in the online supplemental material.

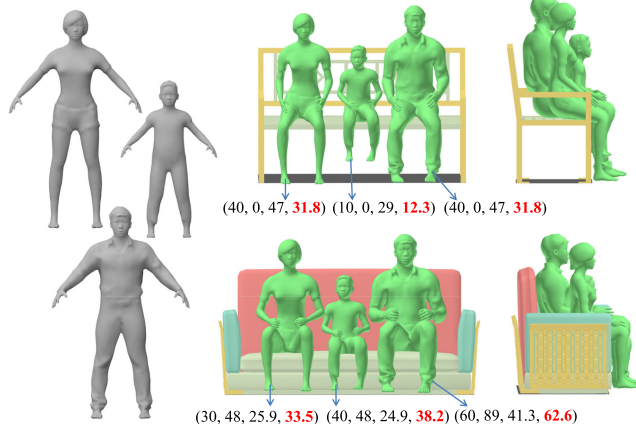


Fig. 15. Virtual fitting for a 3-seater bench and a sofa for a family with ergonomic ratings.

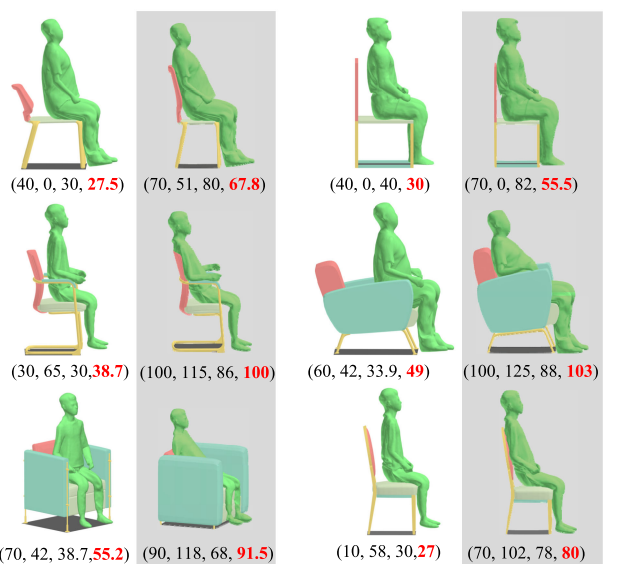


Fig. 16. Chair models with gray background are improved by fitting a higher ergonomic score.

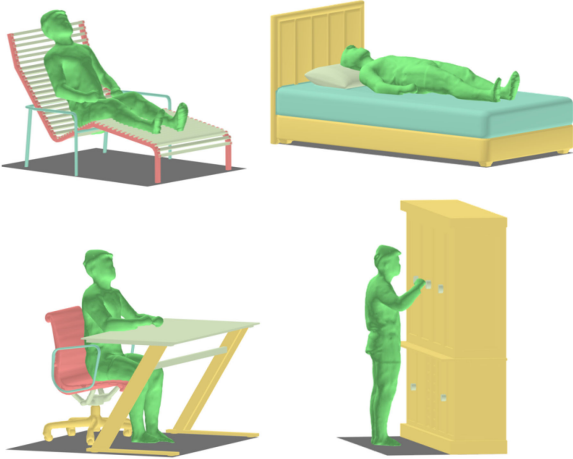


Fig. 17. Our method can deal with other categories of furniture with slight modification.

We further demonstrate an indoor scene of virtual fitting of various furniture models by a family with grandparents, parents, and a child. Fig. 1 depicts that the grandfather sits on a single sofa with support from the backrest, while the armrest is too low to support his arms. The parents sit on the long couch, where the father can incline to touch the backrest, while the mother is not comfortable to be supported by the backrest seeing that the seat-pan depth is much higher than her sitting depth. Grandma and the child sit on the dinner table. The height of the table supports the arms of the grandmother but poorly supports the child's arms. However, the dinner chair does not fit the grandmother whose legs cannot touch the floor. A test of the affordability of various furniture models in the house for an individual family member through the scene of virtual fittings is thus manageable.

## 6.5 Comparison & Discussions

Our method is a pose-induced human shape deformation for virtual fitting of chair models. As mentioned in Section 2, there are a few related work on pose-driven shape analysis [19] and shape reform [28]. However, their research goals are different from ours. Therefore, it is difficult to make a direct comparison based on the same application scenarios. Here, we discuss the difference between our method and the existing work.

Kim et al. [19] aimed to predict a human skeleton pose based on a given shape of object model by predicting contact and end effector probabilities. Zheng et al. [28] aimed to reshape and explore the model collections with respect to a given human skeleton pose, which ranks fitness between the skeleton pose and the object model. As a comparison, our method can evaluate the fitness between the real human shape and the chair model. Fig. 18 shows an application scenario in which different body shapes may have the same stick figure and our method can effectively distinguish them by providing different ergonomic ratings.

*Limitations of our Method.* There are several directions to improve our work. First, our method requires segmented chairs as input. Although it is suitable for chair products in online stores, an automatic segmentation algorithm is highly desired as a preprocess step. Second, our method is designed for working with users dressed with loungewear. Although

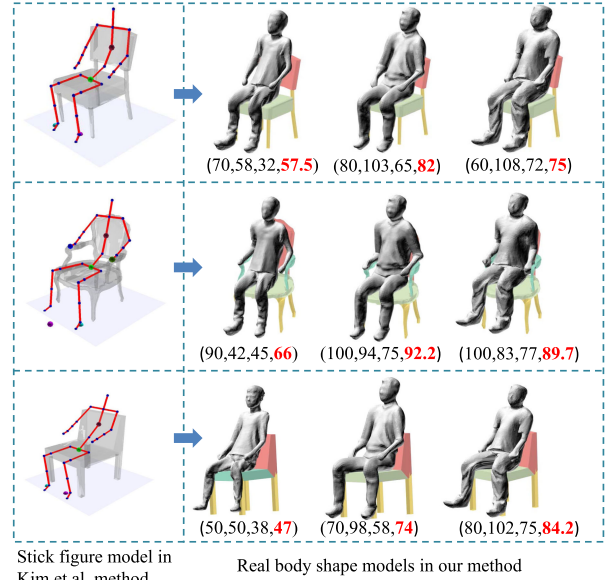


Fig. 18. Comparison of a stick figure model [19] and our method. For different body shapes that have the same stick figure, our method can effectively distinguish them by providing different ergonomic ratings and different rankings.

it is convenient for users, dressing tight-fitting garments can lead to more accurate and robust segmentation. Third, our method is specifically designed for chair evaluation. More types of furniture can be considered in future work.

## 7 CONCLUSION

In this paper, we propose an efficient approach to fit avatars to 3D chairs and then evaluate in terms of ergonomic criteria. Our method uses the real human shape to generate new poses according to the geometrical structure of the chair and contact interactions between the human and chair. Then we deform the pose of the human avatar and align it with the shapes of chair models through utilizing the ergonomic guidelines in the chair design. We propose a quantitative rating for the ergonomic performance of chairs, which indicates the fit extent and comfort of chairs to specific users. A user study and extensive experiments demonstrate that our method works well for a wide range of chairs and can provide good prediction of chair fitness.

## ACKNOWLEDGMENTS

We thank the anonymous reviewers for their constructive comments that help us to improve the paper. This work was supported by the Natural Science Foundation (NSF) of China (61725204, 61521002), NSF of Guangdong Province (2016A030313499), The Science and Technology Planning Project (STPP) of Guangdong Province (2015A030401030) and STPP of Guangzhou City (201804010362).

## REFERENCES

- [1] T. H. Kwok, Y. Q. Zhang, C. C. L. Wang, Y. J. Liu, and K. Tang, "Styling evolution for tight-fitting garments," *IEEE Trans. Vis. Comput. Graph.*, vol. 22, no. 5, pp. 1580–1591, May 2016.
- [2] F. Hahn, B. Thomaszewski, S. Coros, R. W. Sumner, F. Cole, M. Meyer, T. DeRose, and M. Gross, "Subspace clothing simulation using adaptive bases," *ACM Trans. Graph.*, vol. 33, no. 4, pp. 105:1–105:9, 2014.

- [3] Z. Chen, R. Feng, and H. Wang, "Modeling friction and air effects between cloth and deformable bodies," *ACM Trans. Graph.*, vol. 32, no. 4, pp. 88:1–88:8, 2013.
- [4] G. Baciu and W. S.-K. Wong, "Image-based collision detection for deformable cloth models," *IEEE Trans. Vis. Comput. Graph.*, vol. 10, no. 6, pp. 649–663, Nov./Dec. 2004.
- [5] G. Pons-Moll, S. Pujades, S. Hu, and M. J. Black, "Clothcap: Seamless 4d clothing capture and retargeting," *ACM Trans. Graph.*, vol. 36, no. 4, pp. 73:1–73:15, 2017.
- [6] L. Rogge, F. Klose, M. Stengel, M. Eisemann, and M. Magnor, "Garment replacement in monocular video sequences," *ACM Trans. Graph.*, vol. 34, no. 1, pp. 6:1–6:10, 2014.
- [7] R. Broquet, A. Sheffer, L. Boissieux, and M.-P. Cani, "Design preserving garment transfer," *ACM Trans. Graph.*, vol. 31, no. 4, 2012, Art. no. 36.
- [8] S. Hauswiesner, M. Straka, and G. Reitmayr, "Virtual try-on through image-based rendering," *IEEE Trans. Vis. Comput. Graph.*, vol. 19, no. 9, pp. 1552–1565, Sep. 2013.
- [9] P. Guan, L. Reiss, D. A. Hirshberg, A. Weiss, and M. J. Black, "Drape: Dressing any person," *ACM Trans. Graph.*, vol. 31, no. 4, pp. 35:1–35:10, 2012.
- [10] W. Xu, N. Umentani, Q. Chao, J. Mao, X. Jin, and X. Tong, "Sensitivity-optimized rigging for example-based real-time clothing synthesis," *ACM Trans. Graph.*, vol. 33, no. 4, pp. 107:1–107:11, 2014.
- [11] P. Eisert, P. Fechteler, and J. Rurinsky, "3-d tracking of shoes for virtual mirror applications," in *Proc. IEEE Conf. Comput. Vis. Pattern Recognit.*, 2008, pp. 1–6.
- [12] Q. Zhang, Y. Guo, P. Y. Laffont, T. Martin, and M. Gross, "A virtual try-on system for prescription eyeglasses," *IEEE Comput. Graph. Appl.*, vol. 37, no. 4, pp. 84–93, 2017.
- [13] A. Nugraha and M. F. Nasrudin, "Augmented reality system for virtual hijab fitting," in *Proc. Int. Vis. Informat.*, 2015, pp. 454–463.
- [14] H. Wang, J. F. O'Brien, and R. Ramamoorthi, "Data-driven elastic models for cloth: modeling and measurement," *ACM Trans. Graph.*, vol. 30, no. 4, pp. 71:1–71:12, 2011.
- [15] H. Li, E. Vouga, A. Gudym, L. Luo, J. T. Barron, and G. Gusev, "3d self-portraits," *ACM Trans. Graph.*, vol. 32, no. 6, pp. 187:1–187:9, 2013.
- [16] J. Tong, J. Zhou, L. Liu, Z. Pan, and H. Yan, "Scanning 3d full human bodies using kinects," *IEEE Trans. Vis. Comput. Graph.*, vol. 18, no. 4, pp. 643–650, Apr. 2012.
- [17] H. Grabner, J. Gall, and L. J. V. Gool, "What makes a chair a chair?" in *Proc. IEEE Conf. Comput. Vis. Pattern Recognit.*, 2011, pp. 1529–1536.
- [18] R. Hu, M. Savva, and O. van Kaick, "Functionality representations and applications for shape analysis," *Comput. Graph. Forum*, vol. 37, no. 2, pp. 603–624, 2018.
- [19] V. G. Kim, S. Chaudhuri, L. Guibas, and T. Funkhouser, "Shape2pose: Human-centric shape analysis," *ACM Trans. Graph.*, vol. 33, no. 4, pp. 120:1–120:12, 2014.
- [20] R. Hu, O. van Kaick, B. Wu, H. Huang, A. Shamir, and H. Zhang, "Learning how objects function via co-analysis of interactions," *ACM Trans. Graph.*, vol. 35, no. 4, pp. 47:1–47:13, 2016.
- [21] K. Kroemer, *Fitting the Human: Introduction to Ergonomics*, Sixth Edition, Boca Raton, FL, USA: CRC Press, 2008.
- [22] C. C. L. Wang, *Geometric Modeling and Reasoning of Human-Centered Freeform Products*. New York, NY, USA: Springer, 2013.
- [23] C. Berlin and C. Adams, *Production Ergonomics: Designing Work Systems to Support Optimal Human Performance*. London, U.K.: Ubiquity Press, 2017.
- [24] National Occupational Health and Safety Commission, *Ergonomic Principles and Checklists for the Selection of Office Furniture and Equipment*. Australian Government Publishing Service, AGPS Press, 1991.
- [25] B. Shackel, K. Chidsey, and P. Shipley, "The assessment of chair comfort," *Ergonomics*, vol. 12, no. 2, pp. 269–306, 1969.
- [26] S. Hignett and L. McAtamney, "Rapid entire body assessment (reba)," *Appl. Ergonomics*, vol. 31, no. 2, pp. 201–205, 2000.
- [27] S. H. Snook and V. M. Ciriello, "The design of manual handling tasks: Revised tables of maximum acceptable weights and forces," *Ergonomics*, vol. 34, no. 9, pp. 1197–1213, 1991.
- [28] Y. Zheng, H. Liu, J. Dorsey, and N. J. Mitra, "Ergonomics-inspired reshaping and exploration of collections of models," *IEEE Trans. Vis. Comput. Graph.*, vol. 22, no. 6, pp. 1732–1744, Jun. 2016.
- [29] M. Alexa, "Linear combination of transformations," *ACM Trans. Graph.*, vol. 21, no. 3, pp. 380–387, 2002.
- [30] L. Kavan and J. Žárá, "Spherical blend skinning: A real-time deformation of articulated models," in *Proc. Symp. Interactive 3D Graph. Games*, 2005, pp. 9–16.
- [31] L. Kavan, S. Collins, J. Žárá, and C. O'Sullivan, "Geometric skinning with approximate dual quaternion blending," *ACM Trans. Graph.*, vol. 27, no. 4, pp. 105:1–105:23, 2008.
- [32] J. Lin, T. Igarashi, J. Mitani, M. Liao, and Y. He, "A sketching interface for sitting pose design in the virtual environment," *IEEE Trans. Vis. Comput. Graph.*, vol. 18, no. 11, pp. 1979–1991, Nov. 2012.
- [33] J. P. Lewis, M. Cordner, and N. Fong, "Pose space deformation: A unified approach to shape interpolation and skeleton-driven deformation," in *Proc. 27th Annu. Conf. Comput. Graph. Interactive Tech.*, 2000, pp. 165–172.
- [34] X. Shi, K. Zhou, Y. Tong, M. Desbrun, H. Bao, and B. Guo, "Example-based dynamic skinning in real time," *ACM Trans. Graph.*, vol. 27, no. 3, pp. 29:1–29:8, 2008.
- [35] N. Magnenat-Thalmann, A. Lapерри'ere, and D. Thalmann, "Joint-dependent local deformations for hand animation and object grasping," in *Proc. Graph. Interface*, 1988, pp. 26–33.
- [36] Y. Kim and J. Han, "Bulging-free dual quaternion skinning," *Comput. Animation Virtual Worlds*, vol. 25, no. 3/4, pp. 321–329, 2014.
- [37] B. Merry, P. Marais, and J. Gain, "Animation space: A truly linear framework for character animation," *ACM Trans. Graph.*, vol. 25, no. 4, pp. 1400–1423, 2006.
- [38] A. Jacobson and O. Sorkine, "Stretchable and twistable bones for skeletal shape deformation," *ACM Trans. Graph.*, vol. 30, no. 6, pp. 165:1–165:8, 2011.
- [39] T. Mukai, "Building helper bone rigs from examples," in *Proc. 19th Symp. Interactive 3D Graph. Games*, 2015, pp. 77–84.
- [40] B. H. Le and J. K. Hodgins, "Real-time skeletal skinning with optimized centers of rotation," *ACM Trans. Graph.*, vol. 35, no. 4, pp. 37:1–37:10, 2016.
- [41] Y. Wang, S. Asafi, O. van Kaick, H. Zhang, D. Cohen-Or, and B. Chen, "Active co-analysis of a set of shapes," *ACM Trans. Graph.*, vol. 31, no. 6, pp. 165:1–165:10, 2012.
- [42] L. Yi, V. G. Kim, D. Ceylan, I.-C. Shen, M. Yan, H. Su, C. Lu, Q. Huang, A. Sheffer, and L. Guibas, "A scalable active framework for region annotation in 3d shape collections," *ACM Trans. Graph.*, vol. 35, no. 6, pp. 210:1–210:12, 2016.
- [43] Y. Zhou and A. W. Toga, "Efficient skeletonization of volumetric objects," *IEEE Trans. Vis. Comput. Graph.*, vol. 5, no. 3, pp. 196–209, Sep. 1999.
- [44] C. Chen, Y. Zhuang, F. Nie, Y. Yang, F. Wu, and J. Xiao, "Learning a 3d human pose distance metric from geometric pose descriptor," *IEEE Trans. Vis. Comput. Graph.*, vol. 17, no. 11, pp. 1676–1689, Nov. 2011.
- [45] Haworth, *The Ergonomic Seating Guide Handbook*. Holland, MI, USA: Haworth Inc., 2002.
- [46] F. Cosmi, H. Marco, and G. Andrea, "Design parameters influence on office chairs comfort," *Bulletin Appl. Mech.*, vol. 4, no. 16, pp. 123–128, 2009.
- [47] E. T. Scott Openshaw, *Ergonomics and Design: A Reference Guide*. Collingdale, PA, USA: DIANE Publishing Company, 2007.
- [48] X. Shi, K. Zhou, Y. Tong, M. Desbrun, H. Bao, and B. Guo, "Mesh puppetry: Cascading optimization of mesh deformation with inverse kinematics," *ACM Trans. Graph.*, vol. 26, no. 3, 2007, Art. no. 81.
- [49] S. H. Jacobson and E. Yücesan, "Analyzing the performance of generalized hill climbing algorithms," *J. Heuristics*, vol. 10, no. 4, pp. 387–405, 2004.
- [50] R. Zemp, W. R. Taylor, and S. Lorenzetti, "Are pressure measurements effective in the assessment of office chair comfort/discomfort? A review," *Appl. Ergonomics*, vol. 48, pp. 273–82, 2015.
- [51] C. Ionescu, D. Papava, V. Olaru, and C. Sminchisescu, "Human3.6M: Large scale datasets and predictive methods for 3d human sensing in natural environments," *IEEE Trans. Pattern Anal. Mach. Intell.*, vol. 36, no. 7, pp. 1325–1339, Jul. 2014.
- [52] ITU, *ITU-R Recommendation BT.500-11. Methodology for the Subjective Assessment of the Quality of Television Images*. Switzerland, Geneva: International Telecommunication Union, 2002.
- [53] M. Kendall, "A new measure of rank correlation," *Biometrika*, vol. 30, no. 1/2, pp. 81–93, 1938.
- [54] I. F. Ilyas, G. Beskales, and M. A. Soliman, "A survey of top-k query processing techniques in relational database systems," *ACM Comput. Surv.*, vol. 40, no. 4, pp. 11:1–11:58, 2008.



**Aihua Mao** received the BEng degree from Hunan University, in 2002, the MSc degree from Sun Yat-Sen University, in 2005, and the PhD degree from the Hong Kong Polytechnic University, in 2009. He is a associate professor with the School of Computer Science and Engineering, South China University of Technology (SCUT), China. His research interests include physical-based simulation, computer-aided design and computer graphics.



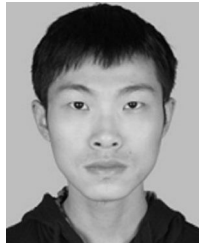
**Hong Zhang** received the BEng degree from South China University of Technology, China, in 2015. He is working toward the MSc student with the School of Computer Science and Engineering, South China University of Technology (SCUT), China. His research interests include computer-aided design and computer graphics.



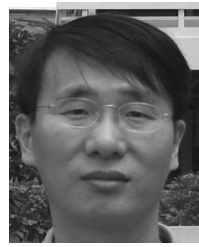
**Minjing Yu** received the BE degree from Wuhan University, China, in 2014 and the PhD degree from Tsinghua University, China, in 2019. She is currently an assistant professor with the College of Intelligence and Computing, Tianjin University, China. Her research interests include computer graphics, cognitive computation and computer vision.



**Yong-Jin Liu** received the BEng degree from Tianjin University, China, in 1998, and the PhD degree from the Hong Kong University of Science and Technology, Hong Kong, China, in 2004. He is a professor with the Department of Computer Science and Technology, Tsinghua University, China. His research interests include computer graphics and computer-aided design.



**Zhenfeng Xie** received the BEng degree from South China University of Technology, China, in 2017. He is working toward the MSc degree in the School of Computer Science and Engineering, South China University of Technology (SCUT), China. His research interest includes computer graphics.



**Ying He** received the bachelor's and master's degrees in electrical engineering from Tsinghua University, in 1997 and 2000, respectively, and PhD degree in computer science from Stony Brook University. He is an associate professor with the School of Computer Engineering, Nanyang Technological University, Singapore. He is interested in the problems that require geometric computing and analysis.

▷ For more information on this or any other computing topic, please visit our Digital Library at [www.computer.org/csdl](http://www.computer.org/csdl).